

## KINEMATIC AND DYNAMIC INVESTIGATION OF A NOVEL INERTIAL PROPULSION DRIVE

<sup>1</sup>Stelica Timofte, <sup>1</sup>Zoltan I. Korka, <sup>2</sup>Attila Gerőcs, <sup>2</sup>Elena S. Wisznovszky (Muncut)<sup>2</sup>, <sup>1</sup>Camelia R. Sfetcu

<sup>1</sup>Babeş-Bolyai University, Doctoral School of Engineering, P-ta Traian Vuia no. 1-4, 320085 Resita, Romania

<sup>2</sup>“Aurel Vlaicu” University of Arad, Automation, Industrial Engineering, Textiles and Transportation Department, B-dul Revoluției no. 77, Arad 310032, Romania,

e-mail: zoltan.korka@ubbcluj.ro

### ABSTRACT

Today there is a great deal of controversy over the operation of inertial propulsion drives (IPD), as they challenge the laws of Newtonian mechanics. Starting with the last decades of the previous century, many devices that use the centrifugal force to generate linear propulsion were patented. Regrettably, whether we are talking about the initial, or the most recent attempts, only a few of these systems passed the patent stage and were involved for practical applications. The aim of this paper is to present an IPD, developed by the authors, which uses for generating linear motion the kinetic energy of several masses, placed in the articulation points of the links of a chain drive. The masses placed equidistantly along the half-length of the chain perform a complex movement, consisting of the specific displacement of the chain elements and a rotation around an axis, that is parallel to the line which joins the centres of the chain wheels. After deducting the equations of the geometric coordinates of the masses, the total propulsion force was computed. The obtained results are supporting the ability of the IPD to generate propulsive force and linear motion.

Keywords: dynamics, inertial force, kinematic, propulsion drive

### 1. INTRODUCTION

In the last decades, countless enthusiastic researchers and inventors have invested a lot of time and efforts to imagine devices able to confront Newtonian mechanics and to develop linear motion by using centrifugal forces. Thus, Allan Jr. [1] asked rhetorically, "Why does classical mechanics forbid inertial propulsion devices when they evidently exist?" Thus, in his book, this author presents some of the functional inertial propulsion drives.

These drives are multi-body systems, their displacement being provided by a propulsive force generated as a reaction to the variable centrifugal force acting on a rotating mass.

Starting from the general equation of the centrifugal force  $F_c$  acting on a rotating body:

$$F_c = m \cdot \omega^2 \cdot R \quad (1)$$

where,  $m$ - the mass of the body,  $\omega$ - the angular speed and  $R$ - the radius of the trajectory, it can be concluded that a time- fluctuating centrifugal force  $F_c(t)$  can be obtained by varying one of the terms on the right-hand side of (1):  $m(t)$ ,  $\omega(t)$  or  $R(t)$ .

Most of the proposed inertial propulsion drives are based on the rotation of several masses on an eccentric trajectory of variable radius. Thus, the “thrust generating device and moving body” proposed by Komora [2] uses two gears to impart a Limaçon-type trajectory (of variable radius) to a mass. Thus, the variable centrifugal force acting on this mass generates a thrust force of the device.

A similar principle is used for the „device for providing propulsion force” developed by Helavuo [3]. As presented in Fig. 1, the device comprises of a mass element (6) and gear for moving the center of gravity of mass (6) around the axis of rotation of an inner gear (2) in such a path (8) in which the centrifugal force provided by mass (6) is higher on the portion (16) of the path (8) than at the second portion (17). In this way, the device generates an asymmetric centrifugal force, which attempts to pull the system.

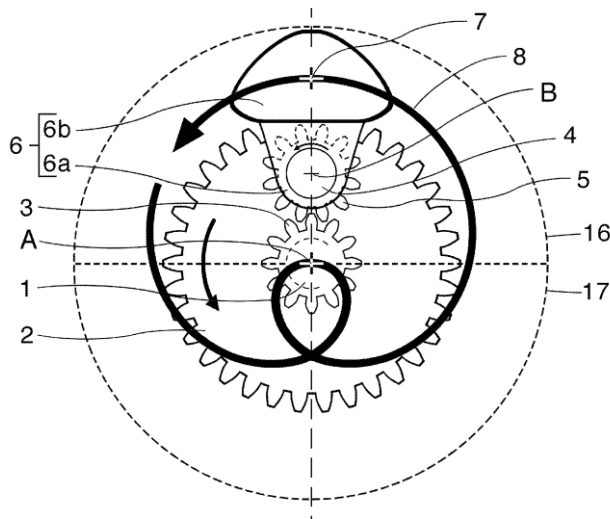


Figure 1. Principle of device for providing propulsion force [2]

Gerocs et al. [4, 5, 6] propose an IPS which generates variable centrifugal force by rotating 8 steel balls along different pseudo-circular trajectories. By means of analytical approach and motion simulation performed in SolidWorks, they conclude that the most advantageous version of the IPS, in terms of velocities, displacements and power consumption, is the version of the retaining disk with cylindrical bore placed eccentric.

The present paper presents a novel propulsion drive developed by the authors, which uses the kinetic energy of equidistant disposed masses, placed in the articulation points of the links of a chain drive, along the half-length of the chain. The masses perform a complex movement, consisting of the specific displacement of the chain elements and a rotation around an axis parallel to the line that joins the centers of the chain wheels.

## 2. PROPOSED INERTIAL PROPULSION DRIVE

The operating principle of the IPD is based on obtaining a variable resultant centrifugal force, which generates an opposite reaction force for the propulsion of the system.

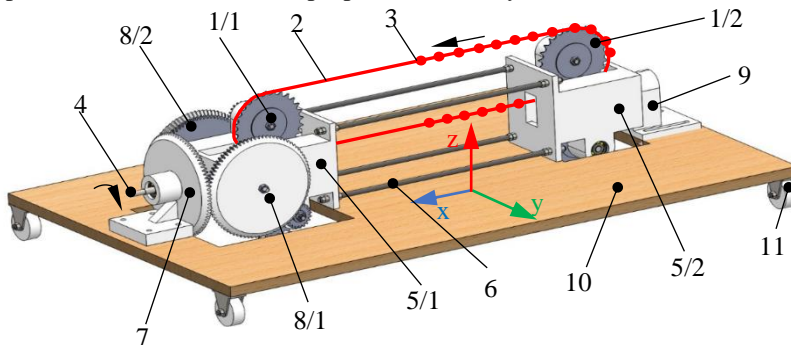


Figure 2. Overview of the IPD

For this purpose, cylindrical steel weights (3) of the same mass are placed on the bolts of a chain (2), on half of its length, on either side of the links. In the same time, the chain drive, having identical wheels (1/1

and 1/2) with  $z = 28$  teeth, is rotating, together with the housings (5/1 and 5/2), around the axis of the driving shaft (4), that is parallel to the line which joins the centres of the chain wheels. The centre distance of the chain drive is  $a = 42 \cdot p$ , where  $p$  is the pitch of the chain. These constructive details ensure a complex movement of the weights which have the peculiarity that, at a complete (pendular) rotation around the axis of the drive shaft, the first two weights placed on the chain reach the starting position. In the same time, the chain wheels are doing four complete rotations. This kinematic connection is ensured by the conical transmission, consisting of a fixed wheel (7), respective two satellite wheels (8/1 and 8/2), and a pair of cylindrical wheels placed inside the housing (8/1) for driving the chain wheel (1/1). The weights of the housings are supported by bearings placed inside the fixed wheel (7) and the support (9), while the centre distance between the chain wheels is maintained constant by 4 threaded rods (6) and hexagon nuts, respectively. The whole assembly is mounted on a rectangular plate (10), supported by four wheels (11). To have a better understanding of the proposed system, Figure 2 provides an overview of the IPD.

### 3. KINEMATIC AND DYNAMIC ANALYSIS OF THE PROPULSION DRIVE

In order to calculate the propulsion force developed by the system, due to the centrifugal forces acting on the masses equal disposed along the half-length of the chain, the kinematic of these masses is investigated. For this purpose, a Cartesian system ( $xOyz$ ) was attached to the plate (10). In addition, it was considered that, in the starting position, the first and last masses are placed in the middle of the centre distance of the chain drive (position A and D in Fig. 3).

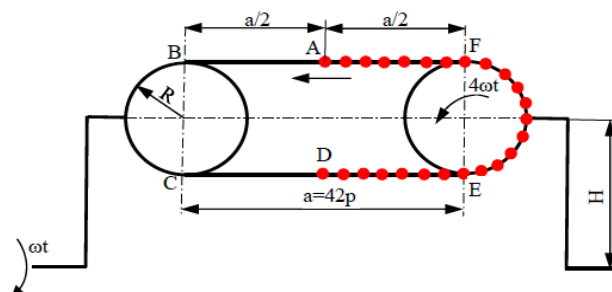


Figure 3. Schematic representation of mass movement

Let's consider  $M$  the total mass of the weights placed in the chain joints.  $M$  can be decomposed into 3 elements ( $M_1$ ,  $M_2$  and  $M_3$ ), which change their shape (linear, respectively arc), value and position of gravity centre, during travelling the route A-B-C-D-E-F-A. The inertial force along the  $y$  axis, generated by the complex movement of the masses attached to the chain can be written as:

$$F_y = \int_0^t \sum_{i=1}^3 M_i(t) \cdot a_{y_i}(t) dt \quad (2)$$

where  $t$  is the time for a complete rotation of the housings around the input shaft axis,  $M_i(t)$  the masses of the  $i=3$  elements and  $a_{y_i}(t)$  the accelerations in  $y$  direction of the  $M_i$  masses.

The first two masses attached to the chain pass through the points A to F, while the driving shaft and the chain wheels rotate with the angles  $\alpha = \omega \cdot t$  and  $\beta = 4 \cdot \omega \cdot t$  respectively ( $\omega$ - angular velocity of the driving shaft), whose values are indicated in Tab. 1.

For the computation of the propulsion force with (2), the masses  $M_1(t)$ ,  $M_2(t)$  and  $M_3(t)$ , respectively the coordinates  $y_1(t)$ ,  $y_2(t)$  and  $y_3(t)$  of the gravity centres of these masses, were determined for each of the 6 characteristic intervals of the angle  $\alpha$  (see Tab. 1).

Table 1. Characteristic angles of the IPD

Point	A	B	C	D	E	F	A
$\alpha$ [rad]	0	$3\pi/8$	$5\pi/8$	$\pi$	$11\pi/8$	$13\pi/8$	$2\pi$
$\beta$ [rad]	0	$3\pi/2$	$5\pi/2$	$4\pi$	$11\pi/2$	$13\pi/2$	$8\pi$

The calculation for the first domain -  $\alpha \in (0, 3\pi/8]$  - was done based on the notations shown in Fig. 4, being presented below, while the calculation results for the other domains are summarized in Tabs. 2 and 3.

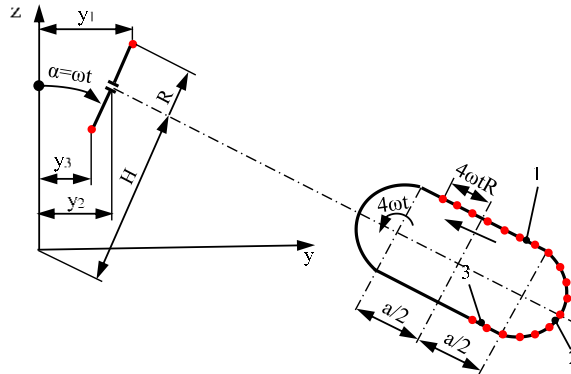


Figure 4. Calculus scheme for the domain  $\alpha \in (0, 3\pi/8]$

The masses  $M_1(t)$ ,  $M_2(t)$  and  $M_3(t)$  are calculated as follows:

$$M_i(t) = \bar{M} \cdot l_i(t) = \begin{cases} \bar{M} \cdot (a/2 + 4\omega t R), & i = 1 \\ \bar{M} \cdot 14p, & i = 2 \\ \bar{M} \cdot (a/2 - 4\omega t R), & i = 3 \end{cases} = \begin{cases} \bar{M} \cdot (21p + 4\omega t R), & i = 1 \\ \bar{M} \cdot 14p, & i = 2 \\ \bar{M} \cdot (21p - 4\omega t R), & i = 3 \end{cases} \quad (3)$$

where  $\bar{M}$  [kg/m] is the linear mass of the weights and R the pitch radius of the chain wheel. The coordinates  $y_1(t)$ ,  $y_2(t)$  and  $y_3(t)$  of the gravity centres of the masses  $M_1(t)$ ,  $M_2(t)$  and  $M_3(t)$  are calculated as follows:

$$y_i(t) = \begin{cases} (H + R) \cdot \sin(\omega t), & i = 1 \\ H \cdot \sin(\omega t), & i = 2 \\ (H - R) \cdot \sin(\omega t), & i = 3 \end{cases} \quad (4)$$

where H is the distance between the axis of the driving shaft and the axis which joins the centres of the chain wheels.

Table 2. Results of masses calculation

Range of $\alpha$	$M_1(t)$	$M_2(t)$	$M_3(t)$
$(0; 3\pi/8]$	$\bar{M} \cdot (21p + 4\omega t R)$	$14\bar{M}p$	$\bar{M} \cdot (21p - 4\omega t R)$
$(3\pi/8; 5\pi/8]$	$\bar{M} \cdot R \cdot (4\omega t - 3\pi/2)$	$42\bar{M}p$	$\bar{M} \cdot [14p - (4\omega t - 3\pi/2)R]$
$(5\pi/8; \pi]$	$\bar{M} \cdot R \cdot (4\omega t - 5\pi/2)$	$14\bar{M}p$	$\bar{M} \cdot [42p - (4\omega t - 5\pi/2)R]$
$(\pi; 11\pi/8]$	$\bar{M} \cdot [21p + (4\omega t - 4\pi)R]$	$14\bar{M}p$	$\bar{M} \cdot [21p - (4\omega t - 4\pi)R]$
$(11\pi/8; 13\pi/8]$	$\bar{M} \cdot R \cdot (4\omega t - 11\pi/2)$	$42\bar{M}p$	$\bar{M} \cdot [14p - (4\omega t - 11\pi/2)R]$
$(13\pi/8; 2\pi]$	$\bar{M} \cdot R \cdot (4\omega t - 13\pi/2)$	$14\bar{M}p$	$\bar{M} \cdot [42p - (4\omega t - 13\pi/2)R]$

**Table 3. Results of coordinate's calculation**

Range of $\alpha$	$y_1(t)$	$y_2(t)$	$y_3(t)$
$(0; 3\pi/8]$	$(H + R)\sin\omega t$	$H\sin\omega t$	$(H - R)\sin\omega t$
$(3\pi/8; 5\pi/8]$	Eq. (5)	$(H + R)\sin\omega t$	Eq. (6)
$(5\pi/8; \pi]$	$(H - R)\sin\omega t$	$H\sin\omega t$	$(H + R)\sin\omega t$
$(\pi; 11\pi/8]$	$(H - R)\sin\omega t$	$H\sin\omega t$	$(H + R)\sin\omega t$
$(11\pi/8; 13\pi/8]$	Eq. (7)	$(H + R)\sin\omega t$	Eq. (8)
$(13\pi/8; 2\pi]$	$(H + R)\sin\omega t$	$H\sin\omega t$	$(H - R)\sin\omega t$

$$y_1 = \left[ H + R \frac{\sin(2\omega t - \frac{3\pi}{4})}{2\omega t - \frac{3\pi}{4}} \cos(2\omega t - \frac{3\pi}{4}) \right] \sin\omega t \quad (5) \quad y_3 = \left[ H + R \frac{\sin(\frac{5\pi}{4} - 2\omega t)}{\frac{5\pi}{4} - 2\omega t} \cos(\frac{5\pi}{4} - 2\omega t) \right] \sin\omega t \quad (6)$$
  

$$y_1 = \left[ H + R \frac{\sin(2\omega t - \frac{11\pi}{4})}{2\omega t - \frac{11\pi}{4}} \cos(2\omega t - \frac{11\pi}{4}) \right] \sin\omega t \quad (7) \quad y_3 = \left[ H + R \frac{\sin(\frac{13\pi}{4} - 2\omega t)}{\frac{13\pi}{4} - 2\omega t} \cos(\frac{13\pi}{4} - 2\omega t) \right] \sin\omega t \quad (8)$$

Calculating the second-order derivative of the coordinates  $y_i(t)$ , the accelerations  $a_{yi}(t)$  of the  $M_i(t)$  masses can be conveniently deduced. The results are summarized in Tab. 4.

**Table 4. Results of acceleration calculation**

Range of $\alpha$	$a_1(t)$	$a_2(t)$	$a_3(t)$
$(0; 3\pi/8]$	$-\omega^2(H + R)\sin\omega t$	$-\omega^2H\sin\omega t$	$-\omega^2(H - R)\sin\omega t$
$(3\pi/8; 5\pi/8]$	Eq. (9)	$-\omega^2(H + R)\sin\omega t$	Eq. (9)
$(5\pi/8; \pi]$	$-\omega^2(H - R)\sin\omega t$	$-\omega^2H\sin\omega t$	$-\omega^2(H + R)\sin\omega t$
$(\pi; 11\pi/8]$	$-\omega^2(H - R)\sin\omega t$	$-\omega^2H\sin\omega t$	$-\omega^2(H + R)\sin\omega t$
$(11\pi/8; 13\pi/8]$	Eq. (9)	$-\omega^2(H + R)\sin\omega t$	Eq. (9)
$(13\pi/8; 2\pi]$	$-\omega^2(H + R)\sin\omega t$	$-\omega^2H\sin\omega t$	$-\omega^2(H - R)\sin\omega t$

$$a_{1,3}(t) = - \left\{ \omega^2 \left[ H + \frac{R\sin(2\theta_{1,3})}{2\theta_{1,3}} \right] + R \frac{\theta_{1,3} [\cos(2\theta_{1,3}) + 2\theta_{1,3} \sin(2\theta_{1,3}) + \dot{\theta}_{1,3} \cos(2\theta_{1,3})] + \theta_{1,3} \sin(2\theta_{1,3})}{\theta_{1,3}^3} \right\} \sin\omega t \quad (9)$$

$$+ \omega R \frac{2\theta_{1,3} \cos(2\theta_{1,3}) - \dot{\theta}_{1,3} \sin(2\theta_{1,3})}{\theta_{1,3}^2} \cos\omega t$$

where  $\theta_1$  is used in the calculus of  $a_1(t)$  and  $\theta_3$  for the calculus of  $a_3(t)$ .  $\theta_1$  and  $\theta_3$  have following values:

$$\theta_1 = \begin{cases} 2\omega t - \frac{3\pi}{4} & \alpha \in (3\pi/8; 5\pi/8] \\ 2\omega t - \frac{11\pi}{4} & \alpha \in (11\pi/8; 11\pi/8] \end{cases}, \quad \theta_3 = \begin{cases} \frac{5\pi}{4} - 2\omega t & \alpha \in (3\pi/8; 5\pi/8] \\ \frac{13\pi}{4} - 2\omega t & \alpha \in (11\pi/8; 11\pi/8] \end{cases} \quad (10)$$

**Table 5. Geometrical characteristics of the IPD**

H [mm]	p [mm]	R [mm]	$\bar{M}$ [kg/m]
70	12,7	56,718	1,003

Further, involving (2) and considering the geometrical characteristics of the IPD, which are described in Tab. 5, the resultant force generated by the system along the y axis where computed for an input speed  $n = 250 \text{ min}^{-1}$  of the driving shaft, which is equivalent to an angular velocity  $\omega = 26,18 \text{ rad/s}$ . The variation of the propulsion force during a complete rotation of the driving shaft is presented in Fig. 5. As one can observe, during the rotation of the drive shaft with an angle of up to  $180^\circ$ , the system generates a positive force, while in the range of  $180-360^\circ$ , the resulting force changes its direction.

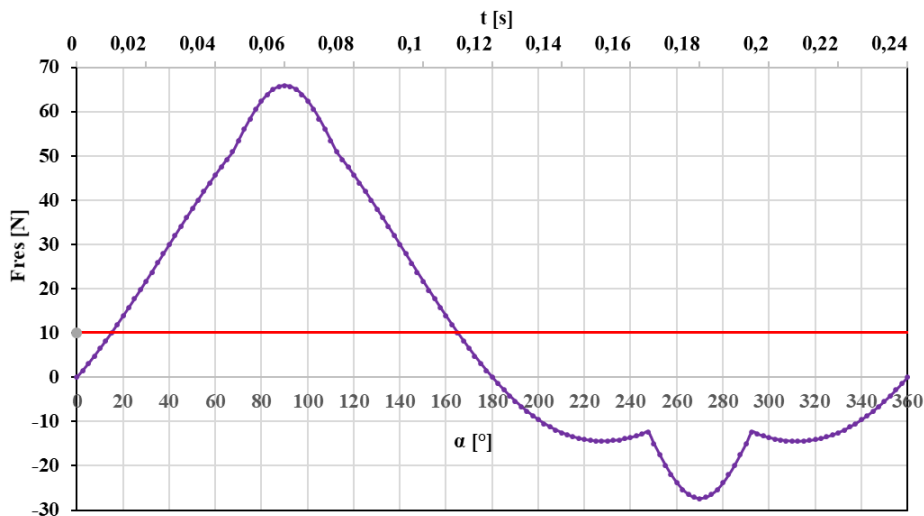


Figure 5. Variation of the propulsion force during a complete rotation of the driving shaft

Even if the resulting force has a fluctuating character, both in terms of size and sense, overall, the system is able to generate a propulsive force, which is plotted as a red line in Fig. 5. This confirms the capability of the IPD to generate linear motion.

## 4. CONCLUSIONS

The paper presents the structure of a novel inertial propulsion drive with masses, which are moving along a complex trajectory. Due to time varying of masses and accelerations of cylindrical weights attached to a chain transmission, the system is generating a one-way inertial force, as a response to the fluctuation of centrifugal force acting on these weights.

Analysing the trajectory of the rotating weights, their masses and coordinates of gravity centres were computed. Finally, the propulsive force generated by the system was deduced.

Based on the analytical approach presented in the paper, it can be concluded that the IPD developed by the authors is functional and capable to generate unidirectional linear movement, being a feasible solution in terms of propulsion on slippery grounds, such as ice or mud, or for spaces where the gravity is missing.

## REFERENCES

- [1] D. P. Allen Jr., Why Does Classical Mechanics Forbid Inertial Propulsion Devices When They Evidently Do Exist?: Is Newtonian Mechanics a Done Deal?, Createspace Independent Pub: Scotts Valley, California, US, 2018.
- [2] M. Komora, Thrust generating device and moving body. Patent no. WO/2001/004491, 2001.
- [3] K. U. Helavuo, Device for providing propulsion force. Patent no. WO/2013/087991, 2012.
- [4] A. Gerocs, Z. I. Korca, I. Biro, V. Cojocaru, Analytical investigation of an inertial propulsion system using rotating masses. Journal of Physics: Conference Series 1426: 012031, 2020.
- [5] A. Gerocs, G. R. Gillich, D. Nedelcu, Z. I. Korca, A multibody inertial propulsion drive with symmetrically placed balls rotating on eccentric trajectories. Symmetry, 2020 12 (9): 1422.
- [6] A. Gerocs, Z. I. Korca, G. R. Gillich, Analytical investigations on the influence of the geometry of an inertial drive on the propulsion force. Annals of "Eftimie Murgu" University from Resita, 2019, 26 (1), pp. 76-85.